Acta Geophysica (2023) 71:1251–1258
https://doi.org/10.1007/s11600-022-00982-6

RESEARCH ARTICLE - APPLIED GEOPHYSICS

Correlation and interpretation of thermal properties of volcanic rocks from Austria

Nina Gegenhuber[1] · **Florian Dertnig**[1]

Received: 22 June 2022 / Accepted: 16 November 2022 / Published online: 8 December 2022

Abstract

Thermal properties of rocks are of great importance not only for geothermal projects. The focus of petrophysical data presented here is laid mainly on volcanic rocks. Thermal properties include not only thermal conductivity but also heat production and heat capacity. A full range of dataset and analysis out of it is presented here. The target of this study is to deliver new insights in the thermal properties of volcanic rocks of Austria. The focus is laid on thermal conductivity—understanding of influencing factors and correlations with other properties, like compressional wave velocity, electrical resistivity or radiogenic heat production. Therefore, a set of data from various volcanic rocks of Austria is presented, analysed in detail and new correlations are presented. The correlations can be further applied on logging data to derive thermal properties in the field. These improved correlations and further interpretations can help in planning geothermal projects and can improve the output of simulations because of the better input data.

Keywords Volcanic rocks · Thermal properties · Correlations

Introduction

Thermal properties of rocks are of great importance not only for geothermal projects. Especially magmatic rocks, which cover a broad range of rocks, which are interesting as geothermal source, are often neglected. The focus of data presented here is laid mainly on volcanic rocks. Thermal properties include not only thermal conductivity but also heat production (out of natural radioactivity data) and heat capacity. Each of these properties has other influencing factors, where thermal conductivity is influenced by mineral composition and pore space whereas heat production by the amount of uranium, thorium and potassium, which are responsible for the natural radioactivity.

In the literature, only a few paper can be found which focus especially on thermal properties of volcanic rocks. Heap et al. (2020) present in their paper thermal conductivity and thermal diffusivity for andesites from New Zealand and Indonesia. Additionally, they present calculations with an effective medium approach and mention the importance of thermal properties for modelling geothermal processes. Mielke et al. (2017) worked with samples from sandstone to carbonates and also with volcanic rocks to find a correlation between thermal conductivity and compressional wave velocity. They show that linear correlations between thermal conductivity and porosity as well as compressional wave velocity work for most of the used rock types. Experimental data are summarized by Büttner et al. (1998) for volcanic rocks in a temperature range from 288 to 1470 K to be applied later on for geoscientific modelling. They do not go into detail about any correlations. Correlations between density, porosity, permeability, compressional and shear wave velocity and thermal conductivity can be found in Mielke et al. (2016) for greywacke and intrusive lavas from the Taupo Volcanic Zone in New Zealand. Data are only plotted against each other with no detailed correlation equations.

The target of this study is to deliver new insights in the understanding of thermal properties of volcanic rocks of Austria. The focus is laid on thermal conductivity—understanding of influencing factors and correlations with other properties. Therefore, a set of data from various volcanic

Edited by Prof. Jadwiga Anna Jarzyna (ASSOCIATE EDITOR) / Prof. Gabriela Fernández Viejo (CO-EDITOR-IN-CHIEF).

✉ Nina Gegenhuber
nina.gegenhuber@unileoben.ac.at

Florian Dertnig
dertnig@furtmueller.eu

[1] Chair of Subsurface Engineering, Montanuniversität Leoben, Erzherzog Johann Street 3, 8700 Leoben, Austria

rocks of Austria is presented, analysed in detail and new correlations are presented. The correlations can be further applied on logging data to derive thermal properties in the field. These improved correlations and further interpretations can help in planning geothermal projects and can improve the output of simulations because of the better input data. The better the input data (especially derived directly in a certain area), the better the output data, which are used for the evaluation of an area of interest, where thermal conductivity is one of those properties, which are of great interest. As input for geothermal process modelling, thermal conductivity is essential.

Samples

Samples are taken at seven different places from outcrops in Austria. Table 1 gives an overview of the places where the samples are collected. All samples are fresh and with no visible alteration. The size of the samples varies (Fig. 1). For the measurements, the samples were cut in shape of a dice, when possible, with a side length of 10 cm for the thermal conductivity and natural radioactivity measurements. Furthermore, plugs have been drilled with a size of 2.5 cm and a length of a bout 2.2 cm. Those plugs are drilled in different directions to make possible anisotropy visible. Having a look on the data, anisotropy is neglected for the interpretation. Therefore, mean values for each sample from the plugs have been calculated.

The basalt from Muehldorf and Kloech shows variable density and porosity, whereas basalt and trachyandesite from Weitendorf, Klausen and Hochstraden show low density and high porosity. Used is additionally to the volcanic rocks, one granite to make differences within the magmatic rocks (plutonic-volcanic types) visible. All these volcanic quarries belong to the age of Neogene. Figure 1 shows some selected examples from the samples taken in the field, cut on two sides for thermal conductivity measurements, and before drilling the plugs.

Table 1 Overview of places where samples are taken

Place	Rock type	Coordinates East	Coordinates North	Comments
Muehldorf	Basalt	15,917	46,934	Variable density and porosity
Weitendorf	Basalt	15,446	46,896	Low density, high porosity
Kloech	Basalt	15,966	46,769	Dense, low porosity
Klausen	Trachyandesite	15,898	46,892	Variable density and porosity
Klausen	Tuff	15,898	46,892	Low density, high porosity
Kloech	Basalt-tuff	15,965	46,769	Low density, high porosity
Hochstraden	Basalt nephelinite	15,926	46,838	Basalt-nephelinite, dense, low porosity
Perg	Granite	14,634	48,259	Mauthausen granite, fine to medium grained

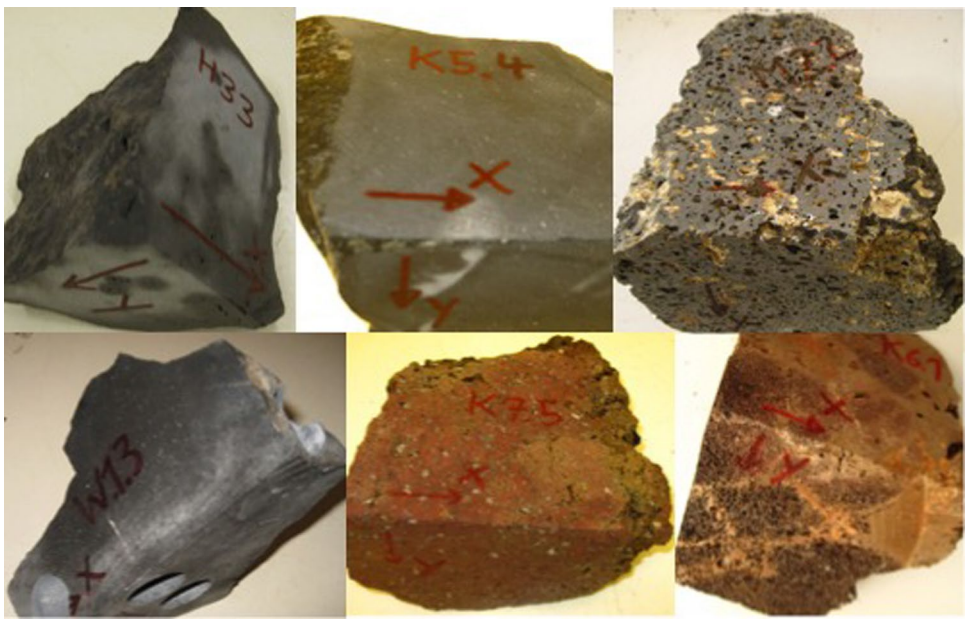

Fig. 1 *H33:* Basalt Nephilinite (Steinbruch Hochstraden); *K5.4:* Basalt (Steinbruch Kloech); *M22:* Basalt-tuff (Steinbruch Muehldorf); *W1.3:* Basalt (Steinbruch Weitendorf); *K7.5:* Red Trachyandesite (Steinbruch Klausen); *K6.1:* Basalt-tuff (Steinbruch Kloech)

Measuring methods

Measured are all relevant petrophysical properties for a full description of rocks: porosity, density (bulk and grain density), compressional and shear wave velocity, electrical resistivity, thermal conductivity, natural radioactivity, heat capacity and permeability in the petrophysics laboratory at Montanuniversitaet Leoben. The following paragraphs explain the singular methods in detail.

The following measurements are carried out on plugs (length: 2 cm, diameter: 2.5 cm). Plugs are taken in different directions to make possible anisotropy visible. Since those samples did not show anisotropy, mean values for each sample of the plug data are taken for the correlations. Figure 2 shows the principal workflow from the sample preparation to the measurements.

Bulk density [g/cm^3] is calculated with measured length and diameter of the cylindrical sample for volume and weight. All of them are measured three times, and the average value is taken. For saturation: samples are put in the desiccator with a vacuum, afterward the water (1 g NaCl/1 l distilled water) is put in and they are stored overnight (minimum of 12 h) under vacuum. Grain density [g/cm^3] is derived from helium pycnometer, and effective porosity is calculated with bulk and grain density. Additionally, effective porosity is determined with principle of Archimedes, where mass is used dry, saturated and under buoyancy. Permeability is measured with a gas permeameter from Vinci Technologies.

Heat capacity [J/kgK] is measured at saturated samples with a self-made calorimeter. Samples are heated up for half an hour with boiling water. Afterward the samples are put in a Dewar vessel with cold water and the temperature increase is measured. Out of these data, the heat capacity can be calculated.

Compressional and shear wave velocity [m/s] were measured with an ultrasonic device at dry and water saturated samples. The signal generator (Geotron, Germany) sends an impulse with 80 kHz via piezoelectric probes through the sample. The signal is further sent to a storage oscilloscope and stored as text file on the computer. The further interpretation is done with a self-made MATLAB code (Gegenhuber and Steiner-Luckabauer 2012).

Specific electrical resistivity [Ohmm] is determined with a 4-electrode array on the saturated samples. Additionally, for the effective porosity calculation and the further correlations with Archie equation (Archie 1942) the conductivity [S/m] of the water is measured with a conductivity meter. Archie equation combines m, the cementation factor [−], R_0 the resistivity of the water saturated formation [Ohmm],

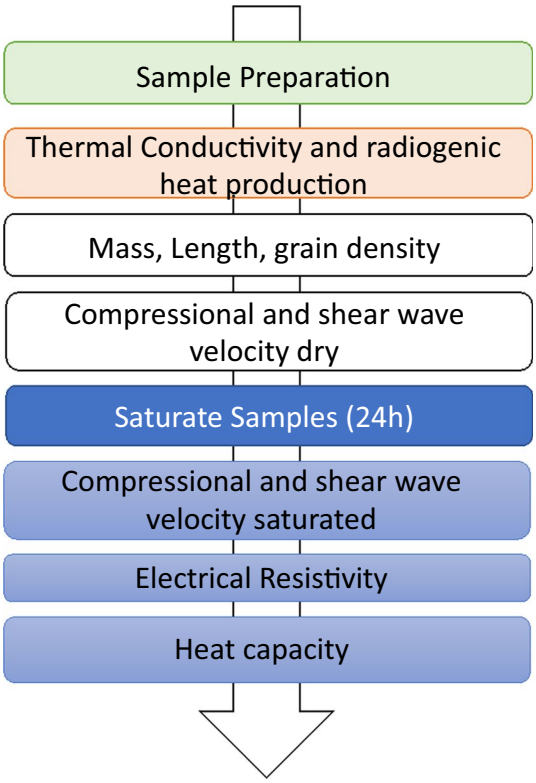

Fig. 2 Overview on the measurement workflow

Φ the effective porosity [−], R_w the resistivity of water [ohm m] and F the formation factor [−].

$$F = \frac{1}{\Phi^m} = \frac{R_0}{R_w} \tag{1}$$

Samples with a low cementation factor show flat or jointed pores. Spherical pores show a higher cementation factor. The formation factor (F) is independent from most rock type (most rock building minerals are isolators).

Thermal conductivity [W/mK] and heat production/natural radioactivity are measured on bigger samples. Thermal conductivity is measured with the TK04 thermal conductivity meter (TeKa, Berlin). Heat production A [HGU or $\mu W/m^3$] is calculated from bulk density [kg/m^3] and natural radioactivity, which is measured with a gammaspectrometer, where the concentration of uranium [ppm] (mainly from Bi_{214}), thorium [ppm] (mainly from Th_{208}) and potassium [%] (from K_{40}) is determined. The used equation is (Buecker and Rybach 1996) the following:

$$A = 10^{-5} * \rho(9.52 * c_U + 2.56 * c_{Th} + 3.48 * c_K). \tag{2}$$

Model calculations

The model calculations for the correlation between thermal conductivity and compressional wave velocity as well as for formation factor from resistivity did already deliver good results for other rock types and a first set of volcanic rocks (Gegenhuber and Kienler 2017; Gegenhuber and Schoen 2012, 2014) and are therefore applied and improved. The following equations with details can be found in the papers mentioned before.

For the calculation of compressional wave velocity, the inclusion model by Budiansky and O'Connell (1976) is used. Thermal conductivity was calculated with the inclusion model by Clausius–Mossotti (Berryman 1995).

The inclusion model by Budiansky and O'Connell (1976) estimates penny-shaped pores and is developed for the calculation of elastic properties. The approach assumes high frequencies for saturated rocks, idealizes ellipsoidal inclusions, isotropic and linear elastic rock matrix and that cracks are isolated with respect to fluid flow.

$$k_{SC} = k_S * \left[1 - \frac{16}{9} * \frac{1 - v_{SC}^2}{1 - 2v_{SC}} * \varepsilon\right] \tag{3}$$

$$\mu_{SC} = \mu_s * \left[1 - \frac{32}{45} * \frac{(1 - v_{SC}) * (5 - v_{SC})}{2 - v_{SC}} * \varepsilon\right], \tag{4}$$

where k_{sc} calculated bulk modulus, k_s bulk modulus host material, μ_{sc} calculated shear modulus and μ_s shear modulus host material.

To calculate the velocity of the compressional wave v_p also the bulk density ρ_b is needed:

$$\rho_b = (1 - \Phi) * \rho_s + \Phi * \rho_{fluid} \tag{5}$$

$$v_p = \left(\frac{k_{SC} + \frac{4}{3} * \mu_{SC}}{\rho_b}\right)^{1/2}, \tag{6}$$

ρ_s grain density from laboratory data, ρ_{fluid} density of the fluid.

For the calculation of thermal conductivity, the equation of Clausius–Mossotti is used:

$$\lambda_{CM} = \frac{1 - 2 * \phi * R_{mi} * (\lambda_S - \lambda_{fl})}{1 + \phi * R_{mi} * (\lambda_S - \lambda_{fl})} \tag{7}$$

$$R_{mi} = \frac{1}{9} * \left(\frac{1}{L_{a,b,c} * \lambda_{fl} + (1 - L_{a,b,c}) * \lambda_S}\right), \tag{8}$$

where λ_S is the thermal conductivity of the matrix, λ_{fl} is the thermal conductivity of the inclusion and R_{mi} is the function of depolarization exponents L_a, L_b, L_c. In this study, the shape of the pores is idealized as plate-like objects ($a = b > > c$). The model assumes inclusions randomly arranged. The input data for the model calculations can be found in Table 2.

Results and interpretation

This chapter gives at the beginning the results of basic properties, like porosity and permeability, which influence thermal properties for a better understanding of data and

Table 2 Overview of the host properties (n = number of samples, k_s = compressional modulus, μ_s = shear modulus, ρ_{matrix} = grain density, λ_s = thermal conductivity) and aspect ratios α and cementation factor m

n	k_s GPa	μ_s GPa	ρ_{matrix} gcm^{-3}	λ_s $Wm^{-1}\,K^{-1}$	α	m
40	65	32	3.00	3.0	0.31	1.5–2

is followed by the correlations and interpretation with the model calculations. In Fig. 3, there is present thermal conductivity dry versus the effective porosity (a) and bulk density (b). The colour discriminates the singular rock types, to make possible petrographic influences visible. All volcanic samples follow the same tendency; this results at first from a comparable mineral composition. Obviously and as assumed, the granite (plutonite) in light blue does not fit to the rest of the volcanic data as result of a different mineral composition. Especially quartz content increases the value with its high thermal conductivity. The expected trend becomes visible: thermal conductivity increases with decreasing porosity and increases with increasing bulk density.

A similar picture can be seen in Fig. 4a, where compressional wave velocity increases with decrease in porosity. Here, the granite does fit to the rest of the data with this trend. Values with higher porosity scatter more. Figure 4b shows an increase in permeability with increase in porosity, but data scatter. No data for granite and volcanic samples

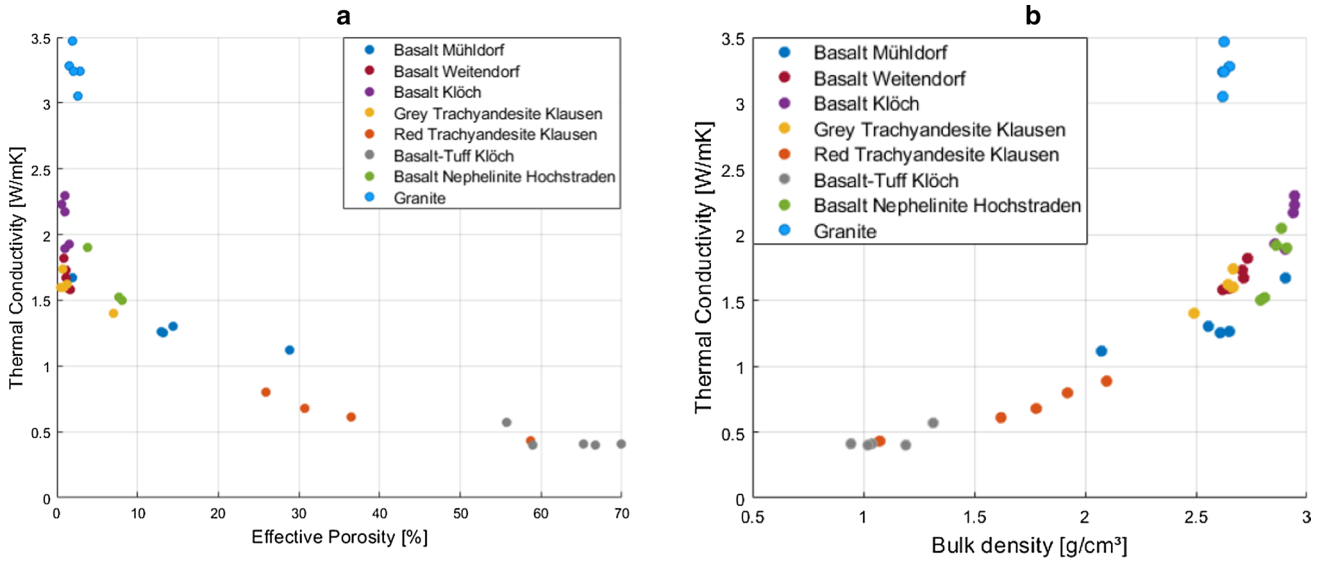

Fig. 3 **a** Thermal conductivity versus effective porosity; **b**: thermal conductivity versus bulk density, colour shows different rock types

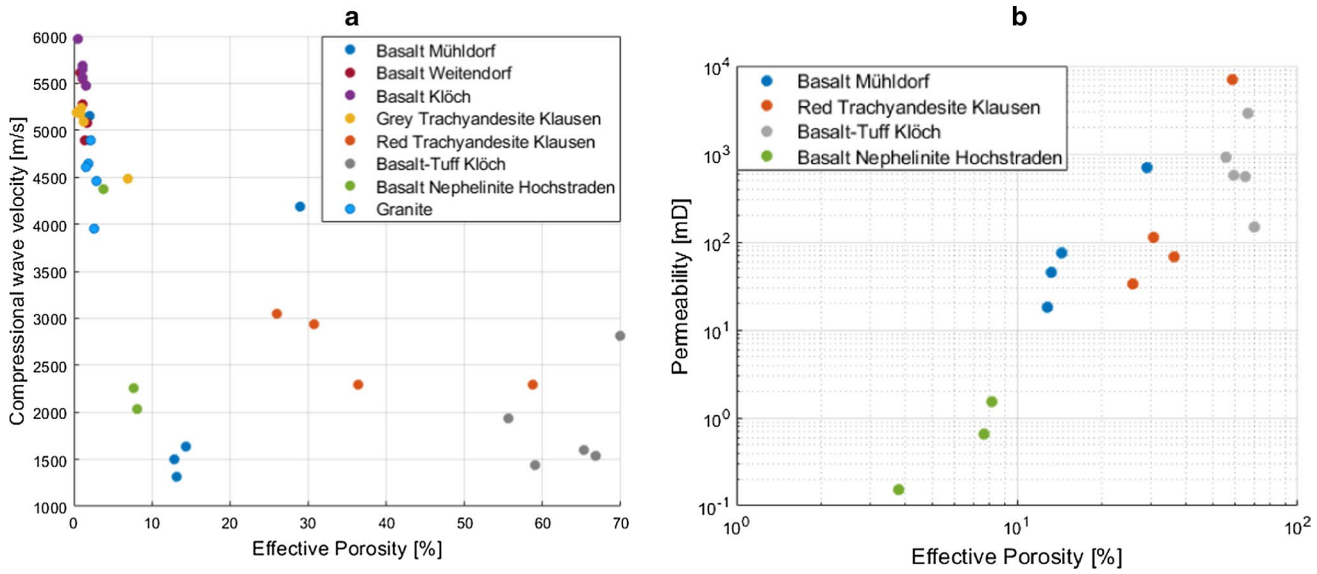

Fig. 4 **a** Compressional wave velocity dry versus effective porosity; **b** permeability versus effective porosity for additional better understanding of data

with low porosity values can be seen here, because permeability was not measurable with the available instrument any more (< 1mD).

Focusing on the correlations for thermal properties we did not take the granite into account anymore. Figure 5a shows again the correlation between thermal conductivity and porosity with no separation focusing on the rock type. Using an exponential correlation line, the result looks good with a regression coefficient $R^2 = 0.95$. The same works good for the correlation between thermal conductivity and bulk density with a $R^2 = 0.97$. Equations can be found summarized in Table 3. Fig. 5b is one outlier visible. This is a granite data. It was expected that this point does not fit to the rest of the data, but to make the petrographic coded influence visible, it was left in the figure.

Up to this point, all regressions are empirical equations. In Fig. 6, the comparison with model derived equations is tested. Figure 6a demonstrates the correlation between thermal conductivity and compressional wave velocity with the correlation equations by Clausius–Mossotti and Budiansky and O'Connell, for the numerical calculation the published excel sheets in Schoen (2011) can be used. Standard correlations, like linear regression or exponential equations, do not deliver good enough results here. The input values for the calculations can be found in Table 2. Results are promising and can reflect data. Figure 6b shows the correlation of thermal conductivity and 1/formation factor^0.5. Also, here data show acceptable good correlations.

The correlation equations can be found in Table 3. These equations give the possibility to be applied on logging data furthermore, if the rock type is known. Sonic log data with compressional wave velocity and resistivity logging data are standard measurements. Therefore, a calculation of thermal conductivity out of these logging data can deliver a big benefit for geothermal projects.

In Fig. 7, the relationship between thermal conductivity and radiogenic heat production is presented. As expected, there is a basic trend visible, with increasing thermal conductivity, natural radioactivity increases. Due to the fact that both of them have other influencing factors: thermal conductivity is influenced by porosity and mineral composition, whereas heat production by bulk density and natural

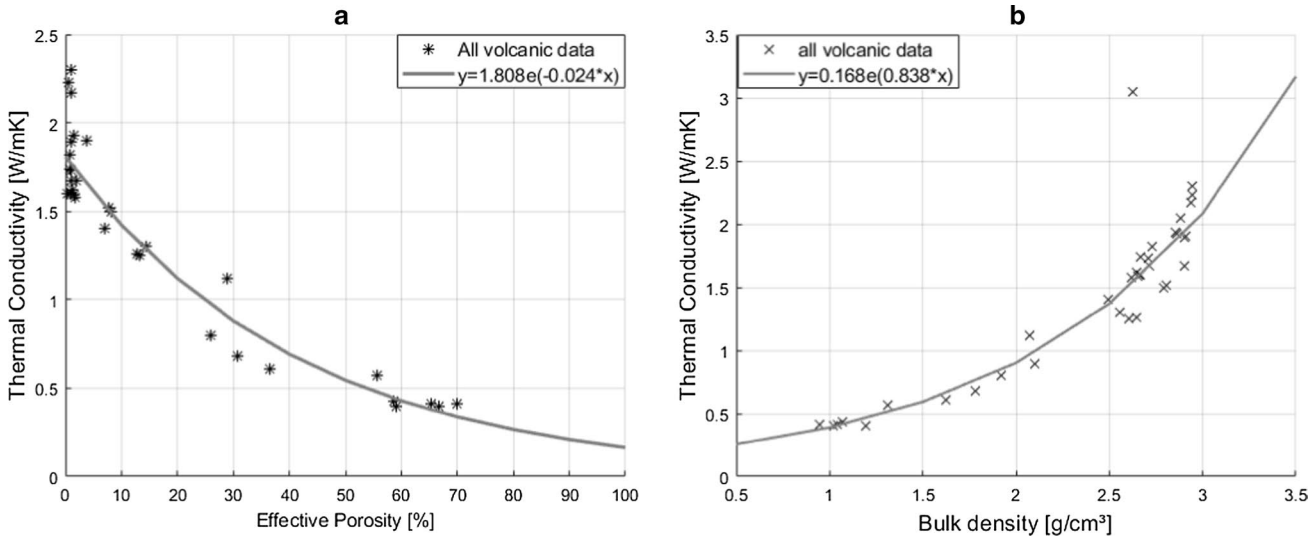

Fig. 5 **a** Thermal conductivity versus effective porosity; **b** thermal conductivity versus bulk density, no separation concerning rock type, excluding granite correlation line with regression coefficient

Table 3 Correlation equations for further application

	Equation	R^2
Effective Porosity (ϕ)—thermal conductivity (λ)	$\lambda = 1.808e\text{^}(-0.024*\Phi)$	0.95
Bulk density (ρ)—thermal conductivity (λ)	$\lambda = 0.168\text{e}\text{^}(0.838*\rho)$	0.97
Thermal conductivity-compressional wave velocity	$\lambda = 1\text{E}{-}07v_p{}^2{-}0{,}0005v_p + 0{,}81$	
Thermal conductivity-1/formation factor^0.5 ($m = 1.5$)	$\lambda = 39{,}62(1/F\text{^}0.5)^2{-}23{,}81(1/F\text{^}0.5) + 2{,}98$	
Thermal conductivity-1/formation factor^0.5 ($m = 2$)	$\lambda = -11{,}466(1/F\text{^}0.5) + 3{,}0775$	
Thermal conductivity-radiogenic heat production (A)	$\lambda = 0.6035*A\text{^}0.7604$	0.623

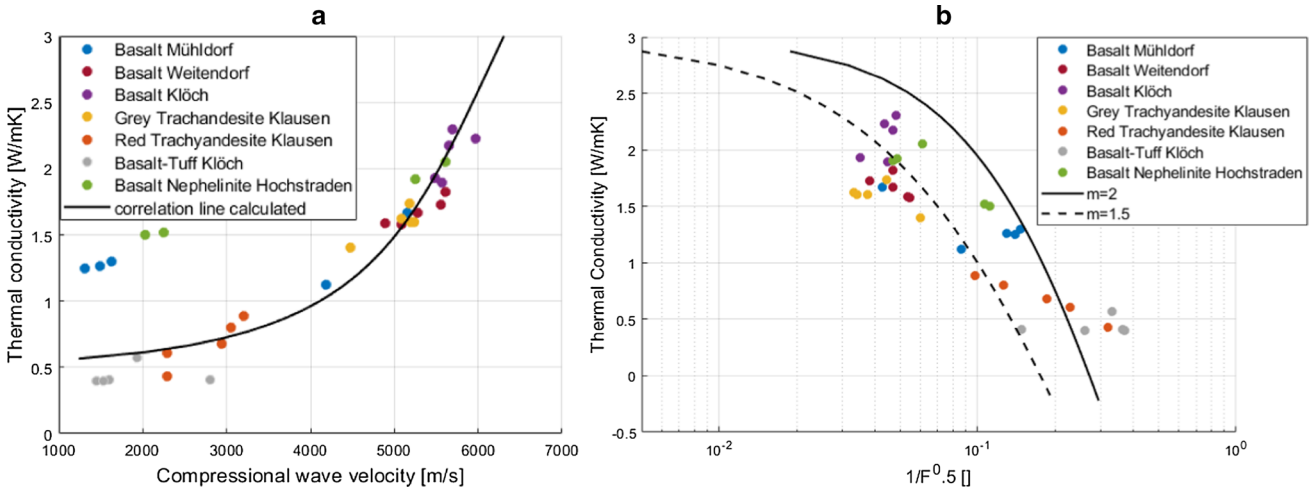

Fig. 6 **a** Thermal conductivity versus compressional wave velocity with the correlation lines derived from model calculations; **b** thermal conductivity versus 1/formation factor^0.5, correlation lines for $m=2$ and $m=1.5$

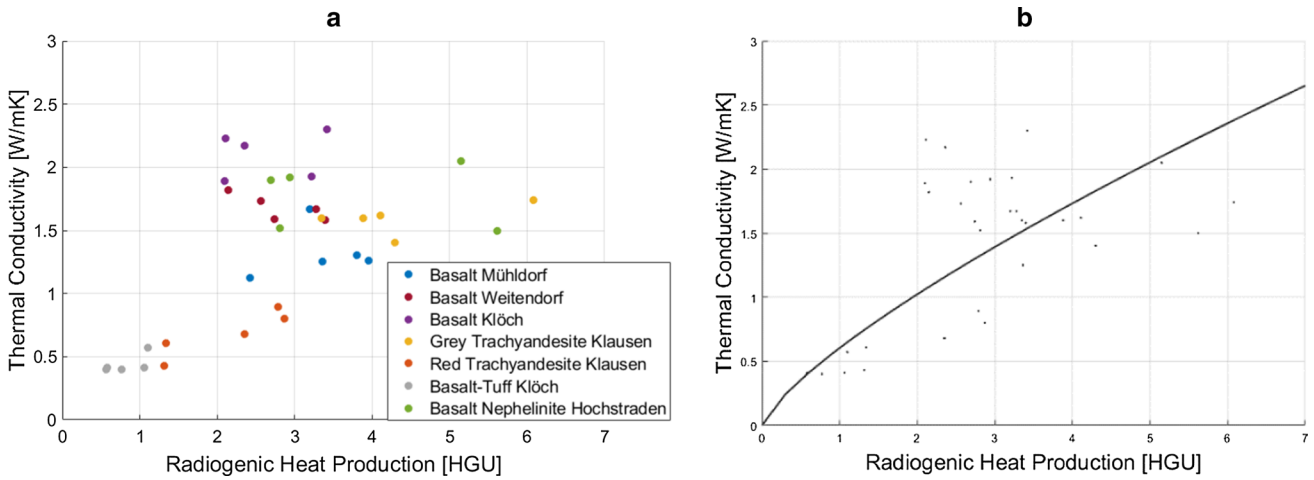

Fig. 7 Thermal conductivity versus radiogenic heat production, **a** with colour after different rock types, **b** no separation but additional correlation ($y=0.6035x^{0.7604}$, $R^2=0.623$)

radioactivity, which depends on the concentration of uranium, thorium and potassium. Displayed is additionally the correlation line with the correlation equation in Table 3.

Figure 8 shows heat capacity versus effective porosity. Heat capacity is mainly dependent on the pore space, as water has a high heat capacity of 4000 [J/kgK] and various minerals around 700–1000 [J/kgK]. Additionally, a correlation equation could be plotted $y=768.3e^{0.0207x}$, $R^2=09{,}822$, when data are not separated using the different rock types.

Conclusion

As thermal properties of volcanic rocks are rarely published, especially as a full set of data for detailed interpretation, this study is a great step forward. Thermal properties, like thermal conductivity, heat capacity and radiogenic heat production, are of great importance not only in geothermal projects. Although various volcanic rocks have been selected here, it becomes obvious that the mineral composition does not vary a lot. The main influencing factors for thermal conductivity

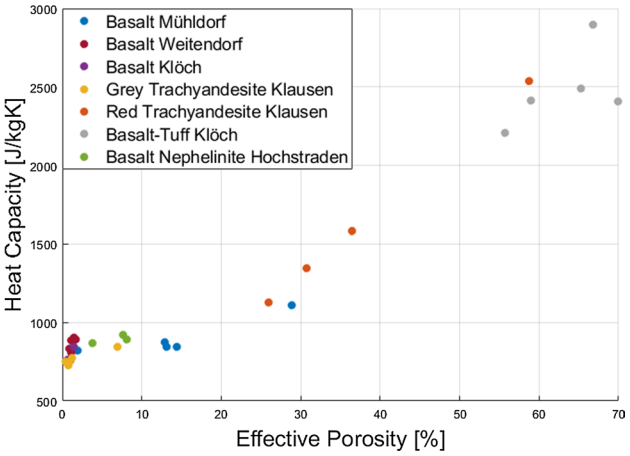

Fig. 8 Heat capacity [J/kgK] versus effective porosity [%], correlation equation for the whole data set: $y = 768.3e^{0.0207x}$, $R^2 = 09{,}822$

is porosity. Therefore, a relatively small data scatter can be observed because of the relative similar mineralogical composition of volcanic rock types. Different mineralogy would (as demonstrated with granite) result in a different position of data clouds. Thermal conductivity increases with decreasing porosity and increasing bulk density as it can be found in the literature. Heat capacity shows higher values with higher porosity, as expected. Radiogenic heat production shows increasing values with increasing thermal conductivity, even the influencing factors vary. Mineral composition is the main influencing factor for thermal conductivity next to porosity and bulk density, whereas radiogenic heat production depends on bulk density and concentration of uranium, thorium and potassium. It seems that for volcanic rocks the main influence is the porosity and bulk density.

Correlations are presented for thermal conductivity with porosity and bulk density as well as radiogenic heat production with empirical equations. Regression coefficient shows high values. Further correlations between thermal conductivity and electrical resistivity are model based. All correlations show good results. The resulting equations can be used for future projects. A further application on standard logging data can deliver information of thermal conductivity in the borehole. This can furthermore improve the quality of geothermal projects.

Acknowledgements This work was supported by the Wissenschaftsfonds FWF [P27929-N29].

Funding Open access funding provided by Montanuniversität Leoben.

Declarations

Conflict of interest The author(s) declare no competing interests.

References

Archie GE (1942) The electrical resistivity log as an aid in determining some reservoir characteristics. Trans Am Inst Miner Met 146:54–62

Berryman J G (1995) Mixture theories for rock properties. In: Rock physics and phase relations, a handbook of physical constants. In: AGU: American Geophysical Union, S. 205–228

Budiansky B, O'Connell RJ (1976) Elastic moduli of a cracked solid. Int J Solids Struct 12:81–97

Buecker C, Rybach L (1996) A simple method to determine heat production from gamma-ray logs. Mar Pet Geol 13:373–375

Buettner R, Zimanowski B, Blumm J, Hagemann L (1998) Thermal conductivity of a volcanic rock material (olivine-melilitite) in the temperature range between 288 and 1470 K. J Volcanol Geotherm Res 80(3–4):293–302. https://doi.org/10.1016/S0377-0273(97)00050-4

Gegenhuber N, Schoen JH (2014) Thermal conductivity estimation from elastic-wave velocity-application of a petrographic-coded model. Petrophysics 55:51–56

Gegenhuber N, Schoen JH (2012) New approaches for the relationship between compressional wave velocity and thermal conductivity. J Appl Geophys 76:50–55. https://doi.org/10.1016/j.jappgeo.2011.10.005

Gegenhuber N, Steiner-Luckabauer C (2012) Vp/Vs automatic picking of ultrasonic measurements and their correlation of petrographic coded carbonates from Austria. 74th EAGE conference & exhibition, Copenhagen

Gegenhuber N, Kienler M (2017) Improved petrographic-coded model and its evaluation to determine a thermal conductivity log. Acta Geophys 65(1):103–118. https://doi.org/10.1007/s11600-017-0010-4

Heap MJ, Kushnir ARL, Vasseur J, Wadsworth FB, Harlé P, Baud P (2020) The thermal properties of porous andesite. J Volcanol Geotherm Res 398(B7):106901. https://doi.org/10.1016/j.jvolgeores.2020.106901

Mielke P, Baer K, Sass I (2017) Determining the relationship of thermal conductivity and compressional wave velocity of common rock types as a basis for reservoir characterization. J Appl Geophys 140(3):135–144. https://doi.org/10.1016/j.jappgeo.2017.04.002

Mielke P, Weinert S, Bignall G, Sass I (2016) Thermo-physical rock properties of greywacke basement rock and intrusive lavas from the Taupo Volcanic Zone, New Zealand. J Volcanol Geotherm Res 324(2):179–189. https://doi.org/10.1016/j.jvolgeores.2016.06.002

Schoen JH (2011) Physical properties of rocks—a workbook. Elsevier, Amsterdam